AD-A064 383 INDIANA UNIV AT BLOOMINGTON DEPT OF CHEMISTRY F/G 20/6
TIME-RESOLVED FLUORIMETRY VIA A NEW CROSS-CORRELATION METHOD,(U)
JAN 79 J M RAMSEY, G M HIEFTJE, G R HAUGEN N00014-77-C-0444

UNCLASSIFIED 3 NL

/ OF /
AD
AO 64383

END
DATE
FILMED
4-79
DDC

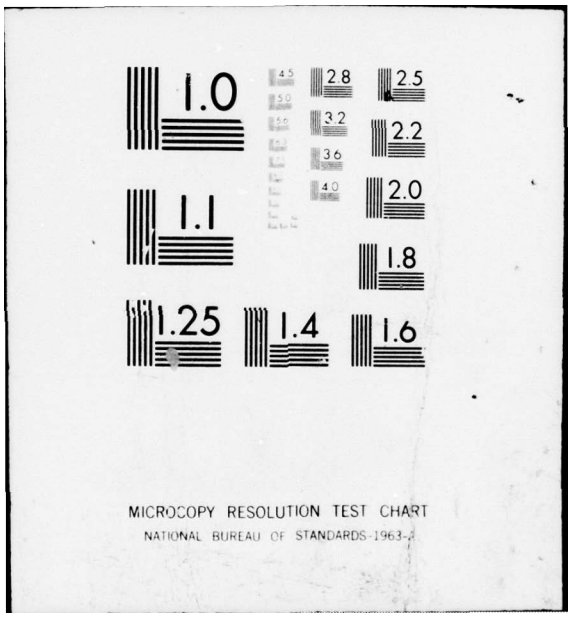
1.0
1.1
1.25
1.4
1.6
1.8
2.0
2.2
2.5
2.8
3.2
3.6
4.0
4.5
5.0
5.6
6.3
MICROCOPY RESOLUTION TEST CHART
NATIONAL BUREAU OF STANDARDS-1963-A

(12) LEVEL II

SECURITY CLASSIFICATION OF THIS PAGE (When Data Entered)

REPORT DOCUMENTATION PAGE

READ INSTRUCTIONS BEFORE COMPLETING FORM

1. REPORT NUMBER: THREE ✓ (14) 31	2. GOVT ACCESSION NO.
3. RECIPIENT'S CATALOG NUMBER	
4. TITLE (and Subtitle): TIME-RESOLVED FLUORIMETRY VIA A NEW CROSS-CORRELATION METHOD	5. TYPE OF REPORT & PERIOD COVERED
	6. PERFORMING ORG. REPORT NUMBER: 3
7. AUTHOR(s): J. M. Ramsey, G. M. Hieftje and G. R. Haugen	8. CONTRACT OR GRANT NUMBER(s): N00014-77-C-0444
9. PERFORMING ORGANIZATION NAME AND ADDRESS: Department of Chemistry, Indiana University, Bloomington, IN 47405	10. PROGRAM ELEMENT, PROJECT, TASK AREA & WORK UNIT NUMBERS: NR 051-659
11. CONTROLLING OFFICE NAME AND ADDRESS: Office of Naval Research, Washington, D. C.	12. REPORT DATE: January 10, 1979
	13. NUMBER OF PAGES: 37
14. MONITORING AGENCY NAME & ADDRESS (if different from Controlling Office) (12) 38p	15. SECURITY CLASS. (of this report): UNCLASSIFIED
	15a. DECLASSIFICATION/DOWNGRADING SCHEDULE

16. DISTRIBUTION STATEMENT (of this Report)

Approved for public release; distribution unlimited

17. DISTRIBUTION STATEMENT (of the abstract entered in Block 20, if different from Report)

18. SUPPLEMENTARY NOTES

Prepared for publication in APPLIED OPTICS

19. KEY WORDS (Continue on reverse side if necessary and identify by block number)

time resolved fluorescence, correlation spectroscopy, mode-locked lasers, laser-induced fluorescence

20. ABSTRACT (Continue on reverse side if necessary and identify by block number)

A new instrument for the measurement of short fluorescence lifetimes is discussed and characterized. The instrument is basically an implementation of the cross-correlation between the excitation source and the induced fluorescence response. Such an approach, with a mode-locked argon-ion laser as the source, is shown to be capable of measuring lifetimes as short as 80ps with a precision of 10ps. The instrument is simpler and less costly than others of similar capability.

DD FORM 1 JAN 73 1473 EDITION OF 1 NOV 65 IS OBSOLETE S/N 0102-014-6601 | UNCLASSIFIED

SECURITY CLASSIFICATION OF THIS PAGE (When Data Entered)

Time-Resolved Fluorimetry via a New Cross-Correlation Method

J. M. Ramsey and G. M. Hieftje[a]

Indiana University

Department of Chemistry

Bloomington, IN 47405

G. R. Haugen

Lawrence Livermore Laboratory

University of California

Livermore, CA 94550

[a]Author to whom correspondence should be addressed.

Time-Resolved Fluorimetry via a New Cross-Correlation Method

Abstract:

A new instrument for the measurement of short fluorescence lifetimes is discussed and characterized. The instrument is basically an implementation of the cross-correlation between the excitation source and the induced fluorescence response. Such an approach, with a mode-locked argon-ion laser as the source, is shown to be capable of measuring lifetimes as short as 80ps with a precision of 10ps. The instrument is simpler and less costly than others of similar capability.

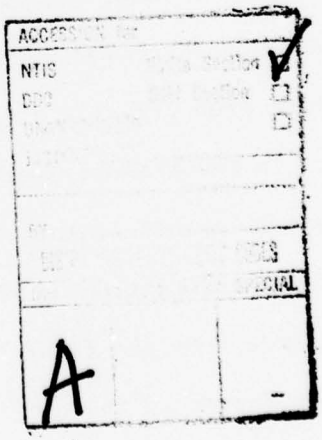

I. Introduction

Time-resolved fluorimetry is an extremely useful tool in a number of branches of science. Not only have fluorimetric methods been instrumental in understanding the photophysics and photochemistry of atoms and molecules[1], but they have also proven useful for elucidating macromolecular properties of biological species[2,3]. Moreover, time-resolved fluorimetry is finding application in qualitative and quantitative chemical analysis[4].

A number of instrumental approaches which exhibit a high degree of temporal resolution have been developed for the determination of fluorescence decay curves. These include time-correlated single-photon systems[5,6], phase shift methods[7,8] and mode-locked laser systems[9,10] utilizing optical gating devices. Of these techniques, the most popular at the present time is the time-correlated single-photon method. This technique has very high sensitivity but is relatively slow in data acquisition and involves relatively complex instrumentation, making it costly to implement. In contrast, phase shift methods are fast but provide at a given source modulation frequency only one measurement point on a decay curve, thereby necessitating an assumed functional form for the decay curve. Finally, laser-based methods offer very high temporal resolution but are costly and often suffer from very low signal-to-noise ratios[9,10].

In the present paper, a new approach for the measurement of fluorescence lifetimes is introduced and characterized. This new approach involves a cross-correlation of the perturbing light impulse with the evoked emission response from the fluorescent species. In this study a CW mode-locked laser serves as the excitation source. The cross-correlation process is implemented in an opto-electronic fashion using high-speed photodetectors

and microwave electronic components. The time-delay variable required by the correlation process is adjusted by means of an optical delay line. This approach has resulted in the development of a time-resolved fluorimeter which provides 10ps time resolution at nanomolar concentration levels while being much less costly to implement and simpler to operate than the earlier approaches mentioned.

II. Description of the Method

The new correlation method can best be understood qualitatively through examination of the instrument designed to implement it. A schematic diagram of the instrument is shown in Fig. 1.

In the instrument a mode-locked laser emits a periodic train of very brief optical pulses. A portion of this radiation is directed into photodiodes PD1 and PD2 by beam splitters BS1 and BS2 respectively. One of these photodiodes, PD1, has a very fast response time and thus can faithfully follow the temporal characteristics of the optical pulse. The output signal from PD1 is sent to a multiplying device, MULT. The portion of the laser radiation transmitted by BS1 and BS2 traverses an optical delay line, consisting of corner-cube reflectors CC1 and CC2, and impinges upon a fluorescence sample in cell C. The fluorescence resulting from this optical stimulus is detected by a photomultiplier tube, PMT. The fluorescence-induced photo-current signal is then sent to the other input of the multiplying device. The output of this multiplier is a signal proportional to the product of the two input signals. The multiplier

output is then sent to a signal processing device which effectively performs a running time average of this product signal.

Operation of the instrument shown in Fig. 1 can be understood intuitively as follows. The optical delay line formed by the movable corner-cube reflectors allows one to change the relative arrival times of the optical pulse at the photodiode, PD1, and the sample cell. By changing this relative arrival time, a temporal offset is generated between the photodiode signal (which mimics the brief laser pulse) and the photomultiplier output (which indicates the fluorescence decay). Because the electrical pulse from the photodiode is considerably shorter in duration than that from the photomultiplier, it serves as a sampling or gating function at the multiplier. In essence, the output of the multiplier is then just a small, time-sampled portion of the photomultiplier signal. In turn, the portion of that signal which is sampled is determined by the position of the corner-cube reflector. The output of the multiplier is then time averaged over many such pulses at a number of selected delay values (i.e., corner cube positions) to provide a precise measurement of the fluorescence decay curve.

The process involved in the foregoing measurement is nothing more than an instrumental computation of the cross-correlation between the laser stimulus and the resultant fluorescence response. With this fact in mind, one can model the behavior of the instrument mathematically as shown below.

In order to determine a fluorescence lifetime from the output of the instrument of Fig. 1, it proves useful first to find the form of the

instrument response function itself. The instrument response function is defined here as that output which the instrument would generate if the photomultiplier observed an optical signal having the temporal characteristics of the laser itself. Such a situation could be created, for example, by placing a scattering suspension in the sample cell. In this case the output of the photomultiplier and the photodiode can be described as the convolution of their respective impulse response functions[11] with the function describing the time dependence of the optical irradiance. The equations describing the temporal output of the photodiode and the photomultiplier, respectively, are

$$D(t) = \int_{-\infty}^{\infty} h_d(\gamma)\, \ell(t-\gamma)\, d\gamma \tag{1}$$

$$P(t) = \int_{-\infty}^{\infty} h_p(\zeta)\, \ell(t-\zeta)\, d\zeta \tag{2}$$

where $h_d(\gamma)$ is the impulse response of the photodiode, $h_p(\zeta)$ is the impulse response of the photomultiplier and $\ell(t)$ is the time-dependent laser irradiance. The overall response for the instrument, $I(\tau)$, can now be written as the cross-correlation of the signals described by Eqs. (1) and (2):

$$I(\tau) = A \int_{-\infty}^{\infty} D(t)\, P(t + \tau)\, dt \tag{3}$$

In Eq. (3), the output of the instrument, $I(\tau)$, is a function of the relative delay parameter, τ. In turn, the value of τ is controlled by the position of the delaying elements of the optical delay line mentioned earlier. In the

above equation, A is a scaling factor which accounts for the gains of the multiplier and the time-averaging device. Combining Eqs. (1), (2), and (3), one obtains

$$I(\tau) = A \int_{-\infty}^{\infty}\int\int h_d(\gamma)\ h_p(\zeta)\ \ell(t - \gamma)\ \ell(t + \tau - \zeta)\ d\zeta d\gamma dt. \tag{4}$$

Integrating Eq. (4) over t yields

$$I(\tau) = A \int_{-\infty}^{\infty}\int h_d(\gamma)\ h_p(\zeta)\ C_{\ell\ell}(\tau + \gamma - \zeta)\ d\zeta d\gamma \tag{5}$$

where $C_{\ell\ell}$ is the optical irradiance autocorrelation function of the laser pulse[12].

Experimentally, $h_d(\gamma)$ approximates a Dirac delta function. Using this fact in Eq. (5) and integrating over γ yields Eq. (6),

$$I(\tau) = A \int_{-\infty}^{\infty} h_p(\zeta)\ C_{\ell\ell}(\tau - \zeta)\ d\zeta. \tag{6}$$

Eq. (6) implies that the output of the instrument when the photomultiplier observes scattering is simply the convolution of the photomultiplier impulse response with the autocorrelation function of the laser pulse. Significantly, Eq. (6) shows no dependence on time, but only on the optical delay parameter, τ.

When the photomultiplier observes fluorescence rather than scattering, the output of the photomultiplier, P'(t), is described by the following equation.

$$P'(t) = \int_{-\infty}^{\infty} F(\nu)\ P(t - \nu)\ d\nu \tag{7}$$

In Eq. (7), $F(\nu)$ is the fluorescence system impulse response function (i.e., the fluorescence decay curve) and P is as described earlier. From Eqs. (1), (2), (3) and (4), the instrument output for the fluorescence experiment, $I'(\tau)$, will be

$$I'(\tau)=A\int_{-\infty}^{\infty}\int\int\int\int h_d(\gamma)\ h_p(\zeta)\ F(\nu)\ \ell(t-\gamma)\ \ell(t+\tau-\nu-\zeta)\ dt\ d\nu\ d\zeta\ d\gamma. \tag{8}$$

As before [cf. Eqs. (3) - (6)], Eq. (8) can be integrated over t and γ, assuming $h_d(\gamma)$ approximates a delta function. This procedure yields

$$I'(\tau)= A\int_{-\infty}^{\infty}\int F(\nu)\ h_p(\zeta)\ C_{\ell\ell}(\tau-\nu-\zeta)\ d\nu d\zeta. \tag{9}$$

Comparing Eq. (9) with Eq. (6) (the latter being the instrument output for a scattering experiment or for fluorescence with a lifetime approximating zero), one observes that the output for the luminescence experiment [Eq. (9)] is just the convolution of the luminescent system impulse response function [$F(\nu)$] with the instrument response function [$I(\tau)$], i.e.

$$I'(\tau) = \int_{-\infty}^{\infty} F(\nu)\ I(\tau-\nu)\ d\nu. \tag{10}$$

Using the foregoing treatment, one can readily formulate a method for determining fluorescence lifetimes with the new instrument. First, the instrument response, $I(\tau)$, can be measured simply by observing scattered laser radiation. Next, $I'(\tau)$ can be determined for the unknown luminescing

substance. The luminescence lifetime can then be readily calculated by deconvolution of $I'(\tau)$ with $I(\tau)$.

Of course, these deductions are limited to the case of only a single exciting pulse of laser radiation. In an actual experiment an "infinite" train of pulses is utilized to perform the correlation operation. Fortunately, the previous treatment can be readily modified to describe this pulse-train situation.

The output from a CW mode-locked laser is a continuous train of optical pulses spaced $\frac{2Ln}{c}$ apart where c is the speed of light, n is the refractive index of the medium within the optical cavity and L is the distance between the two reflectors comprising the cavity. Such a train of pulses can be assumed to be a coherent pulse train, i.e., that all pulses have essentially the same temporal/amplitude characteristics. To mathematically express this pulse train, the optical irradiance function described earlier must be convolved with an infinite sequence of delta functions spaced equally in time

$$\ell_e(t) = \int_{-\infty}^{\infty} \sum_{n=-\infty}^{\infty} \ell(\lambda)\ \delta(t - nT - \lambda)\ d\lambda \qquad (11)$$

where ℓ is as described previously, δ is the Dirac delta function and the subscript e denotes that the optical irradiance function, $\ell_e(t)$, is now a train of the pulses described by ℓ. Also $T = \frac{2Ln}{c}$; i.e., T is the pulse spacing determined by the laser cavity.

To describe the new instrument response function, $I_e(\tau)$, Eq. (11) must be inserted into Eq. (4), which then becomes

$$I_e(\tau) = \lim_{M\to\infty} \frac{A}{2MT} \int_{-\infty}^{\infty}\int_{-\infty}^{\infty}\int_{-\infty}^{\infty}\int_{-\infty}^{\infty}\int_{-MT}^{MT} \sum_{n=-\infty}^{\infty} \sum_{i=-\infty}^{\infty} h_d(\gamma)\, h_p(\zeta)\, \ell(\lambda)\, \ell(\beta)$$

$$\delta(t-nT-\lambda-\gamma)\, \delta(t-iT-\beta-\zeta+\tau)$$

$$d\zeta d\gamma d\lambda d\beta dt. \qquad (12)$$

The $\lim_{M\to\infty} \frac{1}{2MT}$ arises because an infinite pulse train is now being correlated[13], and a time average is being found in Eq. (12) rather than a time integral as in Eq. (4). Of course, to determine $I_e(\tau)$, one cannot afford to do the infinite time average implied by Eq. (12). However, $I_e(\tau)$ will converge to its infinite time average value within a time interval equal to a few cycles of the lowest frequency contained in $\ell_e(t)$. In the present instrument, this frequency is $\frac{1}{T}$ (the reciprocal of the mode-locked pulse train period); accordingly, even the shortest practicable measurement time will produce a value of M large enough to render the approximation valid. Conveniently, τ can assume any value, because the pulse train is essentially of infinite length, and there is no concern with end effects[14].

Performing the time integration in Eq. (12) yields

$$I_e(\tau) = \frac{2MA}{2MT} \sum_{(n-i)=-\infty}^{\infty} \int_{-\infty}^{\infty}\int_{-\infty}^{\infty}\int_{-\infty}^{\infty}\int_{-\infty}^{\infty} h_d(\gamma)\, h_p(\zeta)\, \ell(\lambda)\, \ell(\beta)$$

$$\delta[(n-i)T + \lambda + \gamma - \beta - \zeta + \tau]\, d\zeta d\gamma d\beta d\lambda \qquad (13)$$

where the summation has been interchanged with integration and the 2M implies that the time integration was performed over time 2MT. Integrating Eq. (13) over β, λ and γ and once again assuming that $h_d(\gamma) \to \delta(\gamma)$, one finds

$$I_e(\tau) = \frac{A}{T} \sum_{k=-\infty}^{\infty} \int_{-\infty}^{\infty} h_p(\zeta)\, C_{\ell\ell}(\tau - \zeta + kT)\, d\zeta. \qquad (14)$$

In Eq. (14), k has been substituted for (n - i). Comparing Eqs. (6) and (14), the only difference is that the latter has been scaled by a factor of $\frac{1}{T}$ and that I_e is now a periodic function.

Following the same procedure as before, Eq. (9) becomes

$$I'_e(\tau) = \frac{A}{T} \sum_{k=-\infty}^{\infty} \iint_{-\infty}^{\infty} F(\nu)\, h_p(\zeta)\, C_{\ell\ell}(\tau - \nu - \zeta + kT)\, d\nu d\zeta \qquad (15)$$

for the periodic pulse train. Again substituting Eq. (14) into Eq. (15), one arrives at Eq. (10).

Several important practical points derive from the foregoing treatment. First, for a valid measurement there is no need for the change in delay time $\Delta\tau$ to be larger than T (the period of the pulse train) because the instrument output has this same periodicity in τ. Second, the higher the pulse repetition rate, $1/T$, the greater the signal repetition rate and the larger its magnitude, I_e or I'_e. Third, it is possible that F(t), the fluorescence decay, will be of sufficient duration that it overlaps the next pulse of radiation, implying that information about F(t) will be lost. In practical terms this fact limits the length of lifetimes that can be conveniently measured.

III. Experimental

A. The Instrument

Fig. 1 is a schematic diagram of the instrument used in this work; all components were mounted rigidly on a 3' x 12' optical table. The excitation source utilized in this instrument is a CW mode-locked Ar+ Laser (Model 171-06 Ar+ laser and Model 361 acousto-optic mode-locker, Spectra Physics, Mountain View, CA). The optical pulse train from this laser has a repetition rate of approximately 82 MHz and a resultant pulse spacing of 12.2 ns. Each pulse contains approximately 5nJ of optical energy and has a full duration at half maximum (FDHM) of approximately 150ps under the operating conditions utilized here.

Immediately following the laser output is a mechanical chopper which interrupts the laser beam at a frequency of 33Hz and a duty factor of 12.5 percent. The chopped beam intersects a glass plate (BS1) used as a beam splitter to direct a small portion of the optical energy into a fast photodiode (PD1). The intensity of this reflected beam is adjusted with a neutral density filter (ND1). The light is then focused to a diffraction-limited spot with a glass lens (L1, f = 57mm) and imaged onto PD1. PD1 is a specially constructed Shottky photodiode[15] having an impulse response FDHM of approximately 50ps. PD1 is reverse-biased with a type B (90V) battery. The alignment of this photodiode is quite critical because its active region is an annular ring that is only approximately 10μm wide. Illuminating regions outside of this active annulus causes charge separation outside of the high-electric-field area, resulting in a less-than-optimal time response. Accordingly, PD1 must be positioned exactly at

the focus of lens L1 and its lateral movement adjusted for best performance. For positioning adjustment, PD1 was mounted on a high-precision x, y, z translation stage (Model 420-05, Newport Research Corp., Fountain Valley, CA).

Following BS1 is a second glass plate BS2. BS2 deflects another small fraction of the laser through a focusing glass lens (L2, f = 57mm) onto PD2 (Model XL56, Texas Instruments, Dallas, TX). PD2 is mounted directly onto an SMA bulkhead connector along with approximately .006μf of shunt capacitance. The reverse-bias on PD2 was supplied by two type B batteries in series (180V).

The main laser beam is directed by folding mirrors M1 and M2 toward the variable optical delay line. Both are dielectric-coated to reflect 5145Å radiation at 45° angle of incidence. From M2 the laser beam travels through a variable neutral density filter (VND) which is used to control the optical power reaching the sample cell. The radiation then arrives at the variable delay line, formed by glass corner-cube reflectors CC1 and CC2 (Edmund Scientific, Barrington, NJ). The return beam from CC1, displaced approximately 3cm from the input beam, is folded by the two dielectric-coated mirrors M3 and M4. Exiting the second corner-cube reflector (CC2), the beam travels through glass lens L3(f = 600mm), neutral density filter ND2 and into the sample cell. Corner cubes CC1 and CC2 were selected for the optical delay elements over corner mirrors because they greatly reduce the mechanical tolerances required for the delay line to produce a spatially stationary return (output) beam.

Corner cubes CC1 and CC2 are mounted on optical holders which move independently along an optical rail. The rail is of sufficient length to

allow approximately 1 meter of movement by each corner cube. The resulting total displacement (Δx = 2m) is sufficient to introduce a relative time delay of greater than 12ns, which is equal to the period of both the pulse train and the cross-correlation function. This optical rail is calibrated with a 1mm per division scale which allows one to set easily any delay time between 0 - 12ns with ±5ps accuracy.

The induced sample fluorescence passes through a suitable interference filter (IF) and is detected by an RCA C31024 photomultiplier tube (PMT). This PMT has a biasing circuit which was constructed in our laboratory and operates at -3500V. The biasing circuit is essentially voltage divider (B) suggested by RCA for high-peak-current operation of this tube. However, the circuit was modified for DC coupling by biasing the suppressor grid at approximately -500V with respect to ground and removing the capacitive coupling network.

The electrical signal from the photomultiplier tube is transmitted via RG-58C coaxial cable into the RF port of a microwave mixer (Model ZFM-4, Mini-Circuits, New York, NY). This mixer is of the double-balanced type with a bandwidth of 1.25 GHz and an IF output extending to DC, a feature essential to this application. Into the other (LO) port of the mixer is conducted the signal from the fast Shottky photodiode.

The transmission line connecting the Shottky photodiode to the mixer is comprised of three main components. Connected to the diode is a short piece of RG-58C coaxial cable fitted with SMA cable connectors. This cable then feeds a constant-impedance, variable-length air dielectric coaxial transmission line (Model 874-LK20L, GenRad, Concord, MA), whose

length can be changed by 22cm, corresponding to a time delay of 0.73ns. Following the variable-length line is a broadband (0-8GHz), -6db power splitter (Model 874-TPD, GenRad, Concord, MA). One of the other two ports of this power splitter is terminated into a broadband 50Ω load while the third port goes to the microwave mixer.

All these components of the transmission line between PD1 and the mixer are important in the elimination of reflections of electrical pulses along the line. Because of an impedance mismatch at the mixer, approximately 10 percent of an incident pulse is reflected from the mixer port and returns along the transmission line toward PD1. In turn, the reverse-biased photodiode appears essentially as an open circuit and returns the pulse very effectively toward the mixer. This process will occur repeatedly and leads to a series of pulses rather than a single pulse arriving at the mixer. These pulses will be separated in time by an amount equal to twice the delay time of the transmission line; also, each pulse will be approximately 10 percent of the amplitude of the previously reflected pulse.

These pulses are largely eliminated through careful selection and adjustment of the components in the transmission line. The variable length transmission line allows one to adjust the time required for a pulse to undergo a complete up-and-back reflection cycle. When this time is adjusted to be exactly one pulse-train period, each reflected pulse exactly overlaps the next original pulse, reducing its influence greatly.

The power splitter inserted into the transmission line also reduces the effect of reflected pulses. With the power splitter inserted into the line, half of the voltage of a pulse will be dissipated by the 50Ω load

for each traverse of the transmission line. Thus the amplitude of reflected pulses observed at the mixer port will be lower in amplitude by 4^{-n} for the n^{th} return pulse.

The output of the microwave mixer feeds the signal channel of a lock-in amplifier (Model 840 Autoloc, Kiethley Instruments, Cleveland, OH) which is terminated into a 1MΩ load. The value of this impedance is critical, because it not only determines the load presented to the mixer, but also determines the range of input levels over which the mixer will multiply properly[16].

The reference signal for the lock-in amplifier is obtained from PIN photodiode PD2. The output of the lock-in amplifier is then sent to a strip-chart recorder (Model SR-204, Heath Co., Benton Harbor, MI).

Fig. 1 is consistent with the implementation of Eq. (13) except that lock-in detection rather than time averaging is used on the product signal from the mixer. The equivalence of these two techniques can be seen by inspecting Eq. (12). Specifically, time integration in Eq. (12) is of the form

$$\lim_{T\to\infty} \frac{1}{2T} \int_{-T}^{T} f(t)\, dt. \qquad (16)$$

Clearly, the time average or mean is being found for the time-dependent periodic function f, implying that the DC or Zero Hz component of the mixer output contains the information being sought. That is, the magnitude of the DC component of the signal from the mixer output indicates the magnitude of the cross-correlation function at the particular delay value for which the corner-cube reflectors are positioned. This DC signal

component can be obtained as well from a low-pass filter as from an integrator if measurement speed is not critical. To achieve an equivalent level of performance, the RC time constant for a simple first-order low-pass filter must be approximately 8 times the integration time.

The lock-in detection scheme is essentially a low-pass filter approach except that the detection bandpass has been moved away from zero Hz. Chopping of the signal also reduces drift of the photomultiplier output.

B. Operation of the Instrument

All optical and electronic delays were adjusted so the signals at the mixer from PD1 and PMT overlapped when one of the corner cubes was at its maximum delay and the other slightly less than its maximum delay. Such a configuration allowed a full period of the correlation function to be observed continuously across the most prominent features of the output. The delay, $\tau = 0$, will be defined here to be when the delay line is set for maximum delay. In the actual instrument the two respective signals which overlap at $\tau = 0$ originate from laser pulses which are 3 periods apart or separated by 36ns in time. Because the correlation function is periodic, this temporal offset is immaterial. [This case corresponds to $k = -3$ in Eqs. (14) and (15)].

The laser was typically run at 28 Amps plasma current which produced an average radiant power output of 400mW at 5145Å under mode-locked conditions.

Photodiode PD2, because of its relatively slow response time, can be aligned with a real-time 500MHz oscilloscope (Model 7A19 vertical amplifier

with R7912 transient digitizer, Tektronix, Inc., Beaverton, OR). Once aligned, PD2 is used to trigger the sampling oscilloscope for observing the output of PD1 and also supplies a reference signal for the lock-in amplifier. PD1 was aligned for optimal response with the help of a 75-ps rise time sampling oscilloscope (Model 7T11, 7S11 sampling plug-ins with S-4 sampling head used in R7904 mainframe, Tektronix, Inc., Beaverton, OR). A typical pulse from the Shottky photodiode at the mixer, i.e., after the power splitter, has a peak amplitude of 250mV and FDHM of 200ps (cf. Fig. 2). With the aid of a picoammeter (Model 414S, Kiethley Instruments, Cleveland, OH), the average current from the photomultiplier is adjusted to approximately 20μA with the chopper running. This adjustment is made by changing the variable neutral density wheel (VND) and neutral density filter (ND2).

To generate a cross-correlation function, the optical delay elements were incrementally moved in 50ps steps (0.75cm) from the $\tau = 0$ to the $\tau = -12.2$ns point. Thus, the strip chart recorder displays a series of levels, each indicating the value of the cross-correlation function, Eqs. (14) and (15), at a specific 50ps step. For convenience of display, these levels were re-plotted to form the smooth curves displayed later in this paper.

IV. Results and Discussion

A. Instrument Response Measurements

To test the new instrument's time-resolution capabilities, laser scattering from 0.22μm polystyrene spheres in H_2O was recorded. Through such an experiment, the instrument response [cf. Eq. (14)] can be experi-

mentally determined. Because the optical irradiance autocorrelation function, $C_{\ell\ell}$, is approximately one-tenth the duration of the photomultiplier impulse response h_p, I_c should be approximately equal to h_p. If the assumption is made that these functions are Gaussian in shape, the FDHM of I_e will be less than one percent greater than that of h_p itself.

Fig. 3 compares the photomultiplier response to scattering measured (A) with the correlation approach to that determined with a sampling oscilloscope (B) (τ_r = 75ps). The FDHM indicated by the cross-correlation instrument is 1.21 ns whereas that produced by the sampling oscilloscope trace is approximately 1.15ns. As expected, the cross-correlation result is very nearly the response of the photomultiplier. Significantly, the cross-correlation procedure faithfully portrays details of the photomultiplier response, including the shoulder on the trailing edge of the pulse.

B. Measurement of Fluorescence Lifetimes

As a demonstration of the new instrument, several fluorescence lifetimes were determined. In these experiments, determinations of the instrument response and the response to luminescence were alternately performed. In this way, any variation in laser power or drift in electronics would be apparent. The FDHM of the instrument response was found to be reproducible to ±5ps, indicating that drift is not a significant problem.

1. Convolute-and-Compare Fitting Method

Luminescence lifetimes were obtained from these data by a convolute-and-compare method[1]. That is, a single Heaviside exponential was assumed to be the impulse response of the fluorophore studied. This

function is then convolved with the instrument response and compared with the measured fluorescence response.

The computer-based convolute-and-compare algorithm was an intelligent routine after that discussed by Zimmerman, et al[17]. In this algorithm, the sum of the squares of the residuals between the experimental and calculated curves is minimized; the amplitude and time constant of the exponential impulse response are the adjustable parameters. Briefly, the algorithm adjusts these parameters by finding the total differential of I'_e, the fluorescence response. The residuals for the calculated and experimental curves at each point are set equal to this total differential at each point. The partial derivatives of the I'_e with respect to the fit parameters are next calculated. One than has N equations, where N equals the number of points describing the curves, in two unknowns where the unknowns are the differentials of the fit parameters. A linear least-squares solution of this overdetermined system of equations is performed to yield numbers for the differentials of the fit parameters. These numbers are then used to correct the initial estimates of the lifetime and the amplitude. A new calculated curve is then generated with the corrected parameters which in turn generates new residuals. This procedure can be performed iteratively until the sum of the squares of the residuals reaches a minimum.

It was found here to be important to adjust two additional variables to obtain an acceptable fit. First, a parameter was introduced to shift the calculated fluorescence decay curve toward longer time delays. This time shift arises from the Stokes shift of the fluorescence emission. The higher energy of scattered laser photons yields photoelectrons with

greater translational energies than those produced by the lower energy fluorescence photons. The velocity vector of the photoelectrons collected is predominately directed toward the first dynode in the photomultiplier, the net result being that longer wavelength radiation produces a longer transit time for electrons to reach the anode[18,19]. The two wavelengths observed here (Stokes shift = 85nm) required a shift of 50ps for an optimal fit; in contrast, no time shift is needed if $\Delta\lambda \leq 30$nm.

Another parameter was introduced to enable the DC level of the response curves to be adjusted. This adjustment is necessary because the convolution of a long-lifetime exponential with a train of pulses yields a curve whose minimum is no longer that of the pulse train but is some greater DC level. This effect would ordinarily be seen in the instrument output as well. However, transformer couplings in the microwave mixer eliminates any DC level in the present instrument. This DC adjustment parameter was determined to be important only for fluorescence lifetimes greater than a nanosecond.

Optimal values for the time shift and DC level parameters are found by systematically incrementing them through their domain until a minimum of the least-squares sum is found.

2. Measured Lifetimes

Fig. 4 shows typical cross-correlation plots generated in a fluorescence lifetime determination. In each case the instrument response is shown with the measured and calculated fluorescence response curves. Immediately apparent in the instrument response plot of Fig. 4A is a second pulse located at $\tau \approx 8$ns. This second hump is the reflected signal from

the Shottky photodiode which was mentioned earlier. Fortunately, the reflected pulse does not strongly affect the validity of measured fluorescence lifetimes; the lifetime can be retrieved faithfully by the convolute-and-compare method as long as all portions of the detection system are responding linearly. The primary disadvantage of the appearance of this second pulse is that it makes a log-linear slope estimation[20] difficult even for a relatively long lifetime.

Table I shows a list of the lifetimes determined. A 600nm interference filter, BW = 35nm (Melles Griot, Danbury, CN), was used for spectral selection at the PMT for the first two samples in Table I, whereas a 546nm interference filter, BW = 8.8nm (Ditric Optics, Marlboro, MA), was employed for the last two samples.

The two numbers for each lifetime, listed under LST SQ and DELTA in Table I, represent the values calculated using two different fitting parameters. The parameter LST SQ is the sum of the squares of residuals or normal least-squares criterion. In contrast, the parameter DELTA involves minimization of the sum of the absolute values of the residuals between the experimental and calculated curves divided by the integral of the experimental curve. Both of these fit parameters are widely used[25]. Significantly, the results obtained using the two fit parameters are not greatly different.

3. Validity of Measured Lifetimes

The mean values, $\bar{X}$, and standard deviations, σ, shown in Table I are weighted values obtained from three independent measurements. These weighted values were calculated using the customary expressions[26]

$$\bar{X} = \frac{\sum_{i=1}^{N} \frac{X_i}{M_i}}{\sum_{j=1}^{N} \frac{1}{M_j}} \tag{17}$$

$$\sigma^2 = \frac{\sum_{i=1}^{N} \frac{(\bar{X} - X_i)^2}{M_i}}{\sum_{j=1}^{N} \frac{1}{M_j}} \tag{18}$$

where N is the number of determinations and M_i is the least-squares sum for determination X_i. When the DELTA fit parameter was employed, its square replaced M_i in Eqs. (17) and (18).

Another informative parameter is the standard deviation of a single lifetime determination, σ_τ, which is obtained using the relation[26]

$$\sigma_\tau = \left(\frac{d^2 M}{d\tau^2} \right)^{-\frac{1}{2}} \tag{19}$$

where M is again the least-squares sum. The derivative is found about that value of τ for which M is a minimum. This quantity was calculated both by deriving an explicit expression for σ_τ and also by numerically computing the second difference of M about its minimum. For all samples, σ_τ was on the order of a picosecond, although actual magnitudes range from slightly greater than 1 ps for Rhodamine B to slightly less than 1 ps for the quenched Fluorescein sample. Of course, this number does not define the reliability of finding the true lifetime of a given sample but instead reflects the linearity of the detection system and the amount of noise in a given set of data.

C. Instrument Sensitivity

The sensitivity of the present instrument and its applicability to dilute and/or low-quantum-yield samples is revealed partly by the operating conditions employed in the preceding studies. To avoid saturation of the PMT by fluorescence, the laser irradiance was ordinarily attenuated by two or three orders of magnitude. Moreover, the lock-in detection system was ordinarily set to a relatively insensitive scale. From this source alone, three orders of magnitude greater sensitivity could be obtained. Thus, lifetimes of subnanomolar concentrations of all samples examined here should be determinable with this instrument. The figure of merit typically used to denote sensitivity[1] is the quantum yield-optical density product required to generate a detection-limit signal for a sample of 1 cm path length. Under the conditions used in this investigation, this figure of merit is calculated to be between 10^{-4} and 10^{-5}. Time-correlated single-photon instruments (the most sensitive technique) have figures of merit near 10^{-7} [1].

D. Practicality of the New Method

The new instrument is both simpler and less expensive than others of similar capability. Lifetimes as short as 80ps have been shown to be measurable; lifetimes as long as 50ns should also be measurable, this limitation being due to the periodicity of the pulse train. Lifetime measurements with this instrument also exhibit high precision, being as good as ±10ps for the shorter lifetimes.

The new instrument lends itself well to automation. A microprocessor could control the scanning of the optical time-delay elements while digitizing

the output of the lock-in amplifier. The instrument also avails itself to signal averaging if automation is introduced. Calculating the maximum rate at which the delay elements can be linearly scanned such that the bandwidth of the changing "DC" component from the mixer falls within the -3db bandwidth of the lock-in amplifier low-pass filter allows one to determine the time needed to do a complete τ scan. With the 300ms time constant typically used for the lock-in amplifier, one finds that a complete scan from 0 to 12.2ns can be performed in less than 6 sec. Thus signal averaging could be employed for improving signal-to-noise ratios.

ACKNOWLEDGEMENT

The authors would like to thank L. Steinmetz for the loaning of the fast Shottky photodiode which he constructed and F. E. Lytle for use of the sampling oscilloscope.

CREDIT

Supported in part by the Office of Naval Research, by the National Science Foundation through grant CHE 77-22152 and by the Public Health Service through grant GM24473-01A1. Taken in part from the Ph.D. thesis of J. M. Ramsey.

REFERENCES

1. W. R. Ware, in Creation and Detection of the Excited State, A. A. Lamola, Ed., (Marcel Dekker, New York, 1971), Vol. 1A, p. 213.
2. I. Isenberg, in Biochemical Fluorescence Concepts, R. F. Chen and H. Edelhoch, Eds., (Marcel Dekker, New York, 1975), Vol. 1, p. 43.
3. M. R. Loken, J. R. Gohlke and L. Brand, in Fluorescence Techniques in Cell Biology, A. A. Thaer and M. Sernetz, Eds., (Springer-Verlag, New York, 1973), p. 339.
4. D. M. Rayner and A. G. Szabo, Appl. Opt. 17, 1624 (1978).
5. B. Leskovar, C. C. Lo, P. R. Hartig and K. Sauer, Rev. Sci. Instrum. 47, 1113 (1976).
6. P. R. Hartig, K. Sauer, C.C. Lo and B. Leskovar, Rev. Sci. Instrum. 47, 1122 (1976).
7. R. Spencer and G. Weber, Ann. N.Y. Acad. Sci. 158, 361 (1969).
8. E. R. Menzel and Z. D. Popovic, Rev. Sci. Instrum. 49, 39 (1978).
9. G. Mourou and M. M. Malley, Opt. Commun. 11, 282 (1974).
10. G. Porter, E. S. Reid and C. J. Tredwell, Chem. Phys. Lett. 29, 469 (1974).
11. J. S. Bendat and A. G. Piersol, Random Data: Analysis and Measurement Procedures, (Wiley-Interscience, New York, 1971).
12. N. S. Nahman, Proc. IEEE, 66, 441 (1978).
13. This is another way of writing the correlation function for non-square integrable functions. Normally it is written

$$C_{ij}(\tau) = \lim_{T\to\infty} \frac{1}{2T} \int_{-T}^{+T} i(t)j(t+\tau)dt$$

where both i and j are non-square integrable, such as periodic, functions.

14. Z. Kam, H. B. Shore and G. Feher, Rev. Sci. Instrum. 46, 269 (1975).

15. Designed and constructed by Lloyd Steinmetz, Dept. of Chemistry, Lawrence Livermore Laboratory.

16. R. H. Wilcox, Rev. Sci. Instrum. 30, 1009 (1959).

17. H. E. Zimmerman, D. P. Werthemann and K. S. Kamm, J. Amer. Chem. Soc. 96, 439 (1974).

18. B. Sipp, J. A. Miehe and R. Lopez-Delgado, Opt. Commun. 16, 202 (1976).

19. Ph. Wahl, J. C. Auchet and B. Donzel, Rev. Sci. Instrum. 45, 28 (1974).

20. L. A. Shaver and L. J. Cline-Love, Appl. Spectrosc. 29, 485 (1975).

21. J. M. Harris and F. E. Lytle, Rev. Sci. Instrum. 48, 1469 (1977).

22. I. B. Berlman, Handbook of Fluorescence Spectra of Aromatic Molecules (Academic Press, New York, 1971).

23. G. M. Hieftje, G. R. Haugen and J. M. Ramsey, Appl. Phys. Lett. 30, 463 (1977).

24. R. R. Alfano and S. L. Shapiro, Opt. Commun. 6, 98 (1972).

25. L. A. Shaver and L. J. Cline-Love in Progress in Analytical Chemistry, I. L. Simmons and G. W. Ewing, Eds., (Plenum Press, New York, 1975), Vol. 8, p. 249.

26. H. D. Young, Statistical Treatment of Experimental Data, (McGraw-Hill, New York, 1962).

Table I. Fluorescence Lifetime Results

Sample	Lifetimes (ns)		
	LST SQ	DELTA	Lit. Values
Rhodamine-B 1×10^{-6}M in Ethanol	2.72 ± 0.13	2.79 ± 0.09	2.88[21] 3.2[22]
Rose Bengal 1×10^{-6}M in Ethanol	0.828 ± 0.017	0.847 ± 0.041	0.7[23] 0.9[22]
Fluorescein 2.42×10^{-5}M in H_2O with 0.01M NaOH and 0.8M KI	0.348 ± 0.010	0.349 ± .010	0.39[7]
Erythrosin-B 1×10^{-6}M in H_2O	0.082 ± 0.017	0.083 ± 0.018	0.11[10] 0.09[24]

CAPTIONS

Figure 1. Schematic diagram of cross-correlation instrument. BS1 and BS2-beam splitters; ND1 and ND2-neutral density filters; PD1 and PD2-photodiodes; M1, M2, M3 and M4 dielectric-coated mirrors; VND-variable neutral density filter; CC1 and CC2-corner cubes; C-fluorescence sample cell; BD-beam stop; IF-interference filter; PMT-photomultiplier tube; LS-microwave line stretcher; PS-microwave power splitter; MULT-microwave mixer; L_1, L_2, L_3-lenses; term-50-Ω microwave load.

Figure 2. Time-dependent output of Shottky photodiode when illuminated with mode-locked argon-ion laser. Measured with sampling oscilloscope, τ_r = 75ps.

Figure 3. Comparison of New Correlator with Sampling Oscilloscope Measurement. A. Output of cross-correlation instrument for detection of a laser pulse. B. Sampling oscilloscope display of laser pulse.

Figure 4. Fluorescence Decay Curves Obtained with New Correlation Lifetime Fluorimeter. A. Rhodamine-B lifetime determination (1×10^{-6}M in EtOH, τ = 2.77ns). Earliest broken peak is instrument response function. Later broken peak is experimental fluorescence decay curve. Solid curve is calculated decay curve. B. Same as A, but for Disodium Fluorescein (2.42×10^{-5}M in H_2O with 0.01M NaOH and 0.8M KI, τ = 0.36ns).

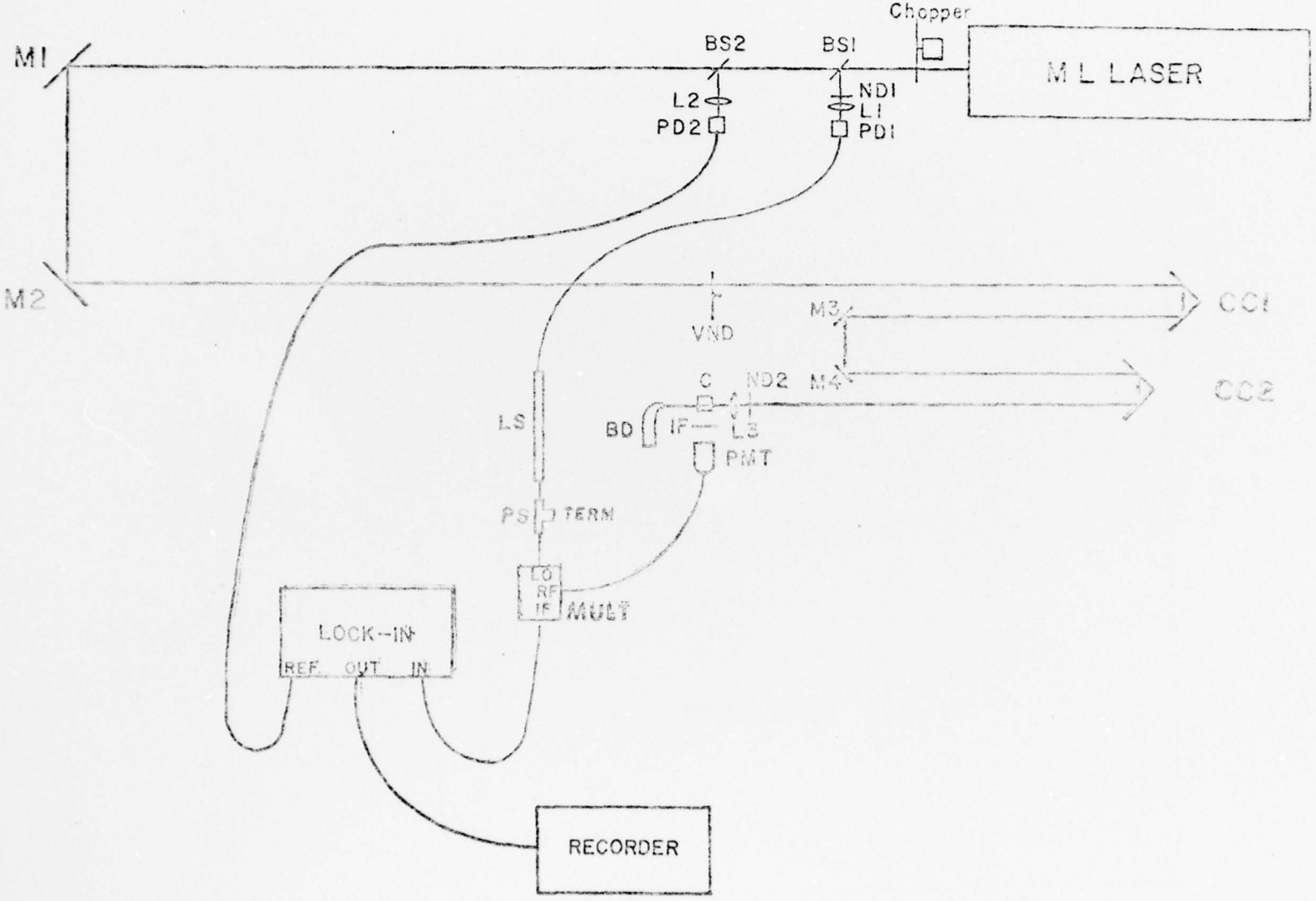
Chopper
M1
BS2
BS1
M L LASER
L2
PD2
NDI
LI
PDI
M2
VND
M3
CC1
C
ND2
M4
CC2
LS
BD
IF
L3
PMT
PS
TERM
LO
RF
IF
MULT
LOCK-IN
REF. OUT IN
RECORDER

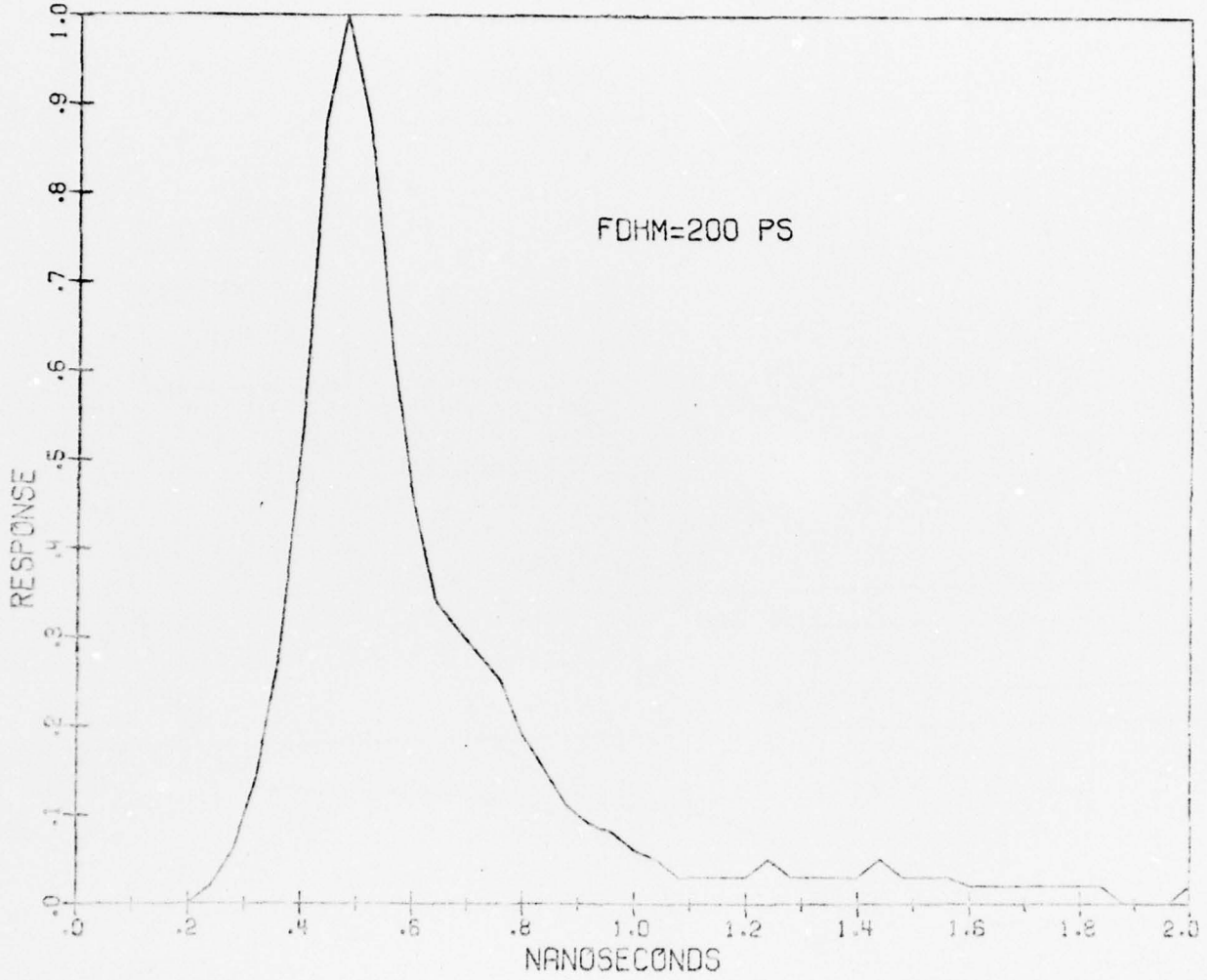
FDHM=200 PS
RESPONSE
0.0
.1
.2
.3
.4
.5
.6
.7
.8
.9
1.0
.0
.2
.4
.6
.8
1.0
1.2
1.4
1.6
1.8
2.0
NANOSECONDS

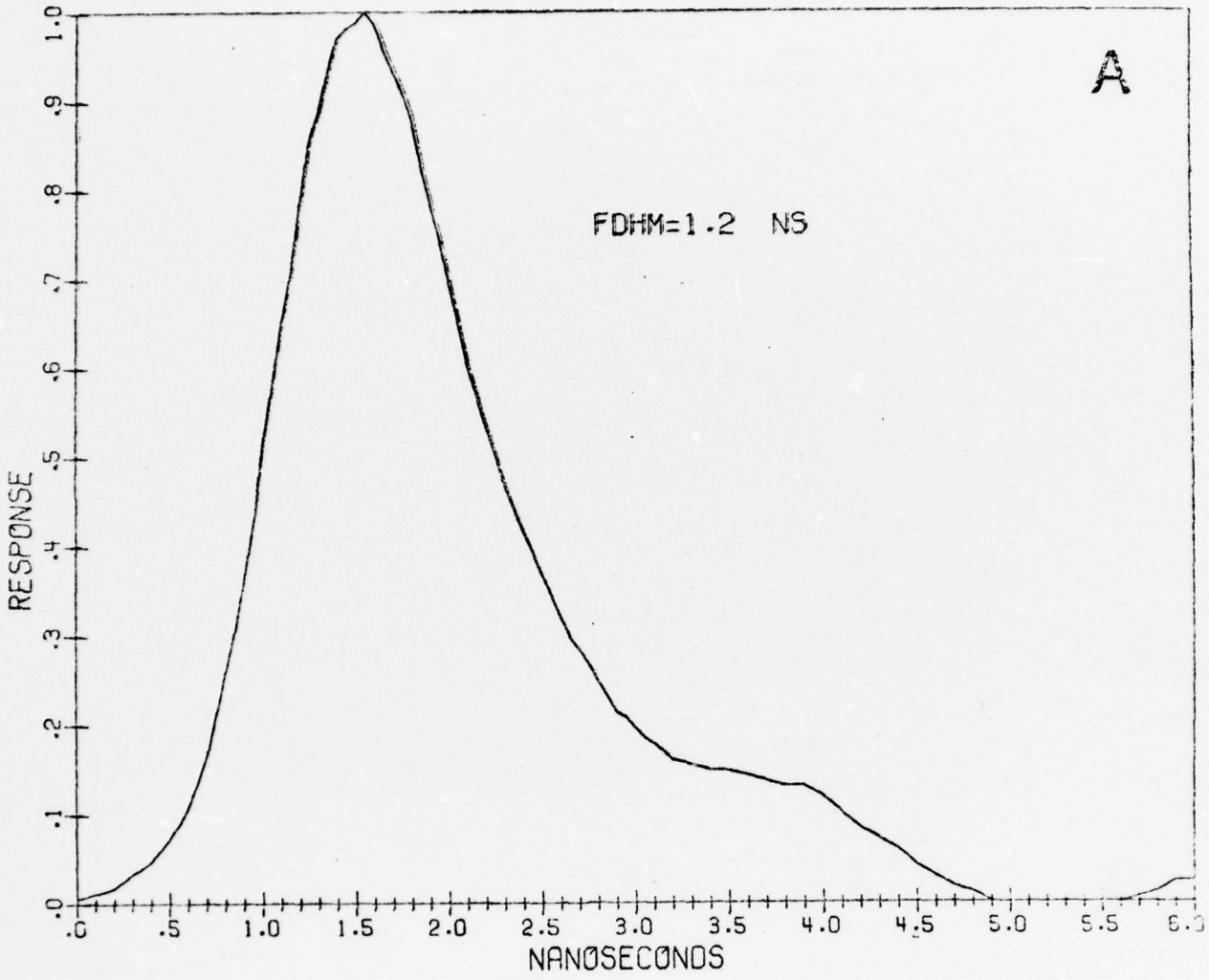
A
FDHM=1.2 NS
RESPONSE
0.0
.1
.2
.3
.4
.5
.6
.7
.8
.9
1.0
.0
.5
1.0
1.5
2.0
2.5
3.0
3.5
4.0
4.5
5.0
5.5
NANOSECONDS

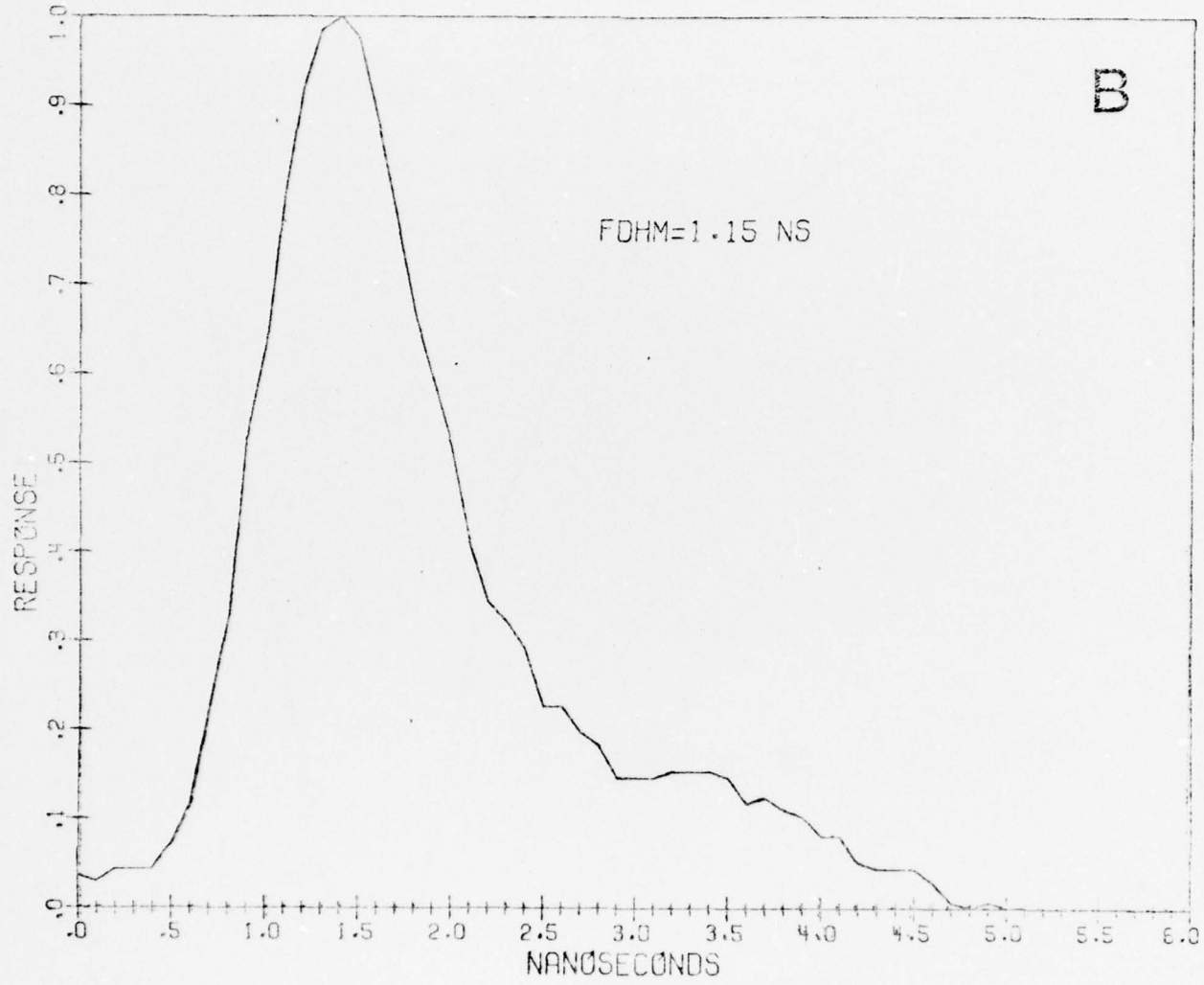
B
FDHM=1.15 NS
RESPONSE
.0
.1
.2
.3
.4
.5
.6
.7
.8
.9
1.0
.0
.5
1.0
1.5
2.0
2.5
3.0
3.5
4.0
4.5
5.0
5.5
6.0
NANOSECONDS

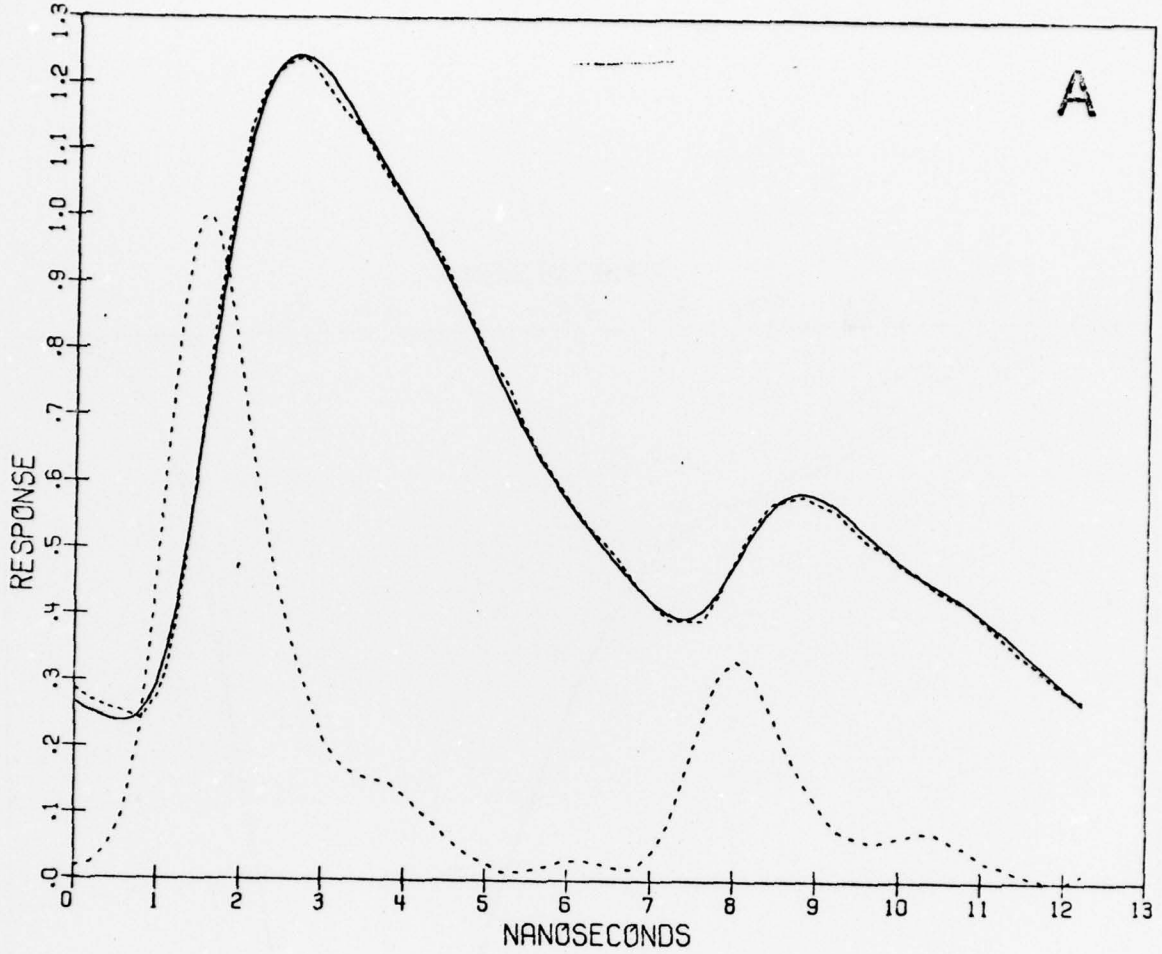
A
RESPONSE
.0
.1
.2
.3
.4
.5
.6
.7
.8
.9
1.0
1.1
1.2
1.3
0
1
2
3
4
5
6
7
8
9
10
11
12
13
NANOSECONDS

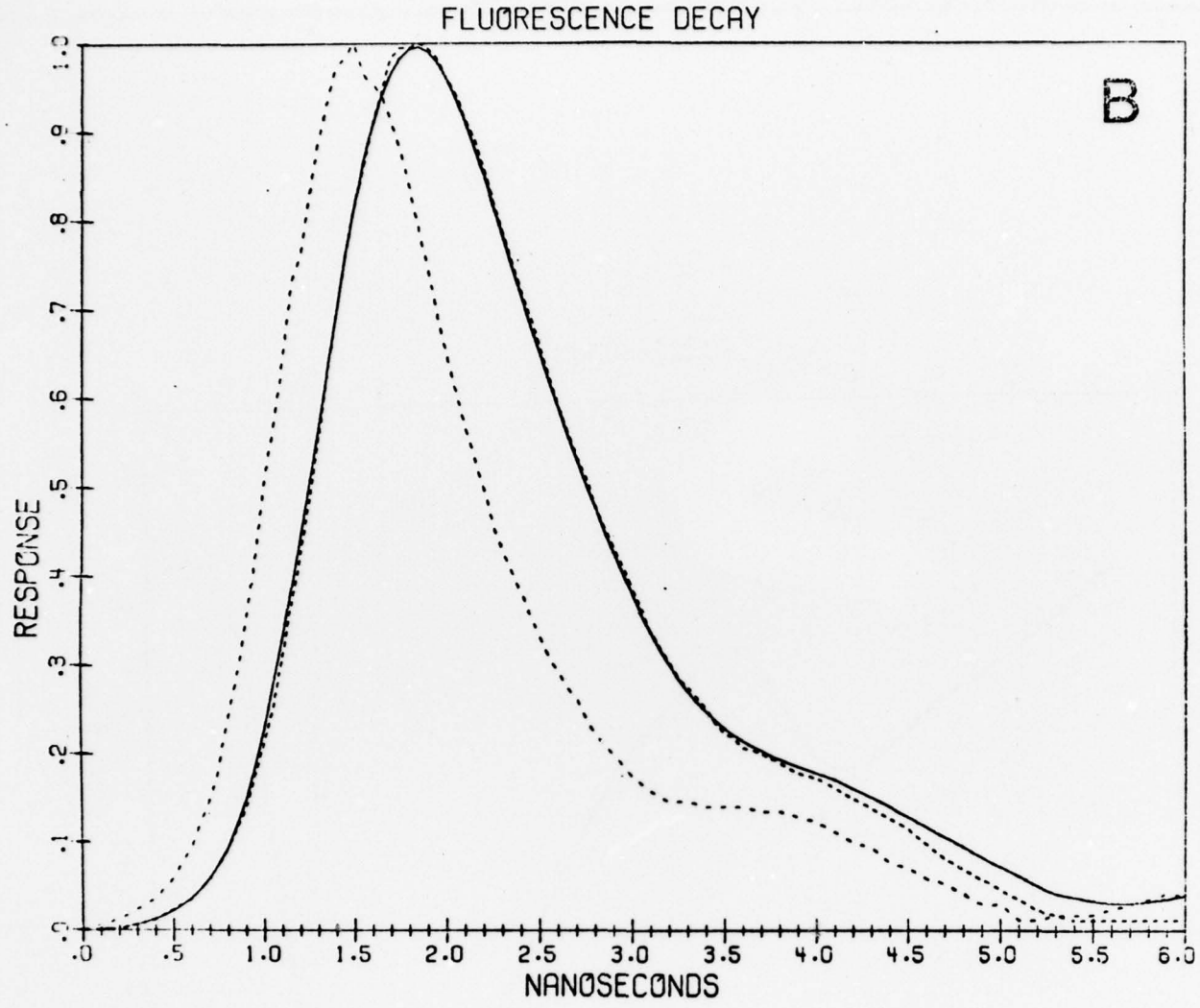
FLUORESCENCE DECAY
B
RESPONSE
.0
.1
.2
.3
.4
.5
.6
.7
.8
.9
1.0
.0
.5
1.0
1.5
2.0
2.5
3.0
3.5
4.0
4.5
5.0
5.5
6.0
NANOSECONDS

472:CAN:716:tsm
78u472-608

TECHNICAL REPORT DISTRIBUTION LIST, GEN

	No. Copies
Office of Naval Research 800 North Quincy Street Arlington, Virginia 22217 Attn: Code 472	2
ONR Branch Office 536 S. Clark Street Chicago, Illinois 60605 Attn: Dr. George Sandoz	1
ONR Branch Office 715 Broadway New York, New York 10003 Attn: Scientific Dept.	1
ONR Branch Office 1030 East Green Street Pasadena, California 91106 Attn: Dr. R. J. Marcus	1
ONR Area Office One Hallidie Plaza, Suite 601 San Francisco, California 94102 Attn: Dr. P. A. Miller	1
ONR Branch Office Building 114, Section D 666 Summer Street Boston, Massachusetts 02210 Attn: Dr. L. H. Peebles	1
Director, Naval Research Laboratory Washington, D.C. 20390 Attn: Code 6100	1
The Assistant Secretary of the Navy (R,E&S) Department of the Navy Room 4E736, Pentagon Washington, D.C. 20350	1
Commander, Naval Air Systems Command Department of the Navy Washington, D.C. 20360 Attn: Code 310C (H. Rosenwasser)	1
Defense Documentation Center Building 5, Cameron Station Alexandria, Virginia 22314	12
U.S. Army Research Office P.O. Box 1211 Research Triangle Park, N.C. 27709 Attn: CRD-AA-IP	1
Naval Ocean Systems Center San Diego, California 92152 Attn: Mr. Joe McCartney	1
Naval Weapons Center China Lake, California 93555 Attn: Dr. A. B. Amster Chemistry Division	1
Naval Civil Engineering Laboratory Port Hueneme, California 93401 Attn: Dr. R. W. Drisko	1
Professor K. E. Woehler Department of Physics & Chemistry Naval Postgraduate School Monterey, California 93940	1
Dr. A. L. Slafkosky Scientific Advisor Commandant of the Marine Corps (Code RD-1) Washington, D.C. 20380	1
Office of Naval Research 800 N. Quincy Street Arlington, Virginia 22217 Attn: Dr. Richard S. Miller	1
Naval Ship Research and Development Center Annapolis, Maryland 21401 Attn: Dr. G. Bosmajian Applied Chemistry Division	1
Naval Ocean Systems Center San Diego, California 91232 Attn: Dr. S. Yamamoto, Marine Sciences Division	1

Encl 1

TECHNICAL REPORT DISTRIBUTION LIST, 051C

	No. Copies
Dr. M. B. Denton University of Arizona Department of Chemistry Tucson, Arizona 85721	1
Dr. R. A. Osteryoung Colorado State University Department of Chemistry Fort Collins, Colorado 80521	1
Dr. B. R. Kowalski University of Washington Department of Chemistry Seattle, Washington 98105	1
Dr. S. P. Perone Purdue University Department of Chemistry Lafayette, Indiana 47907	1
Dr. D. L. Venezky Naval Research Laboratory Code 6130 Washington, D.C. 20375	1
Dr. H. Freiser University of Arizona Department of Chemistry Tuscon, Arizona 85721	
Dr. Fred Saalfeld Naval Research Laboratory Code 6110 Washington, D.C. 20375	1
Dr. H. Chernoff Massachusetts Institute of Technology Department of Mathematics Cambridge, Massachusetts 02139	1
Dr. K. Wilson University of California, San Diego Department of Chemistry La Jolla, California	1
Dr. A. Zirino Naval Undersea Center San Diego, California 92132	1
Dr. John Duffin United States Naval Postgraduate School Monterey, California 93940	1
Dr. G. M. Hieftje Department of Chemistry Indiana University Bloomington, Indiana 47401	1
Dr. Victor L. Rehn Naval Weapons Center Code 3813 China Lake, California 93555	1
Dr. Christie G. Enke Michigan State University Department of Chemistry East Lansing, Michigan 48824	1
Dr. Kent Eisentraut, MBT Air Force Materials Laboratory Wright-Patterson AFB, Ohio 45433	1
Walter G. Cox, Code 3632 Naval Underwater Systems Center Building 148 Newport, Rhode Island 02840	1